Heliyon 9 (2023) e21780

Contents lists available at ScienceDirect

Heliyon

journal homepage: www.cell.com/heliyon

Research article

MHD blood flow effects of Casson fluid with Caputo-Fabrizio fractional derivatives through an inclined blood vessels with thermal radiation

Dzuliana Fatin Jamil [a], Salah Uddin [b], Mohsin Kazi [c], Rozaini Roslan [d,*], M.R. Gorji [e], Mohd Kamalrulzaman Md Akhir [f,g]

[a] Department of Mathematical Sciences, Faculty of Science, Universiti Teknologi Malaysia, 81310 Johor Bahru, Johor, Malaysia
[b] Department of Humanities & Science, College of Aeronautical Engineering, National University of Sciences & Technology, Risalpur, 23200, Pakistan
[c] Department of Pharmaceutics, College of Pharmacy, POBOX-2457, King Saud University, Riyadh 11451, Saudi Arabia
[d] Faculty of Applied Sciences and Technology, Universiti Tun Hussein Onn Malaysia, Pagoh Campus, 84600 Muar, Johor, Malaysia
[e] Faculty of Medicine and Health Science, Ghent University, 9000 Ghent, Belgium
[f] Faculty of Engineering Technology, Universiti Tun Hussein Onn Malaysia, Pagoh Campus, 84600 Muar, Johor, Malaysia
[g] ANNA Systems LLC, Moscow Region, Dubna, 9 Maya Street, Building 7B, Building 2 Office 10.141707, Moscow, Dolgoprudnenskoe Highway, 3, Fiztekhpark, Moscow 141980, Russia

A B S T R A C T

This study investigates a fractional-order time derivative model of non-Newtonian magnetic blood flow in the presence of thermal radiation and body acceleration through an inclined artery. The blood flow is formulated using the Casson fluid model under the control of a uniformly distributed magnetic field and an oscillating pressure gradient. Caputo-Fabrizio's fractional derivative mathematical model was used, along with Laplace transform and the finite Hankel transform technique. Analytical expressions were obtained for the velocity of blood flow, magnetic particle distribution, and temperature profile. These distributions are presented graphically using Mathcad software. The results show that the velocity increases with the time, Reynolds number and Casson fluid parameters, and diminishes when Hartmann number increases. Moreover, fractional parameters, radiation values, and metabolic heat source play an essential role in controlling the blood temperature. More precisely, these results are beneficial for the diagnosis and treatment of certain medical issues.

1. Introduction

The research of biofluid flow in the presence of magnetic field known as biomagnetic fluid dynamics (BFD) is a crucial topic of investigation into how fluid flow behaves when influenced by magnetic fields. Numerous researchers have been involved to this branch of fluid dynamics [1], [2], [3], [4] due to the wide range of applications that bioengineering and medical science have proposed, including studies on magnetic tracers, selective drug delivery utilising magnetic particles as drug carriers. Furthermore, magnetic hyperthermia also could be used to treat cancer. [5] proposed the concept of investigating the magnetic and electrical properties of blood under a single mathematical model. [6] examined a theoretical formulation for the flow of blood through the inclined artery with the presence of magnetic field. [7] examined the effects of body acceleration on Herschel-Bulkley model of pulsatile blood flow via an inclined stenotic artery with the effects of slip velocity.

For the past three decades fractional-order derivatives have been limited to the work by mathematicians. Recently, fractional calculus has been applied in other domains as well due to the vast applications to many real-world problems. [8] introduced another

* Corresponding author.
E-mail addresses: mkazi@ksu.edu.sa (M. Kazi), rozaini@uthm.edu.my (R. Roslan), mohammad.rahimigorji@ugent.be, m69.rahimi@yahoo.com (M.R. Gorji).

https://doi.org/10.1016/j.heliyon.2023.e21780
Received 13 March 2023; Received in revised form 23 October 2023; Accepted 27 October 2023

Available online 4 November 2023

derivative technique followed by theoretical and applied studies in a lot of practical applications. [9] carried out blood flow analysis in cylindrical tube with the presence of transverse magnetic, magnetic particles and oscillatory pressure gradient. [10] performed an analysis of electro-magneto blood flow along with magnetic particles through a circular channel subject to an electric and a uniform external magnetic field. [11] provided a comparative study of non-steady flows of a second-degree fluid with Newtonian heating and time-fractional derivatives, namely Caputo and Caputo-Fabrizio. Given the growing interest for modelling using fractional derivatives, multiple fractional derivatives models have been developed based on existing fluid models [12], [13], [14], [15] and [16].

While blood flow with heat transfer is primarily an essential use in biomedical area, many researchers [17], [18], [19], [20] and [21] have successfully applied their concepts to explore a variety of knowledge about how heat transfer occurs. Heat transport requires many complex processes in tissues such as tissue heat conduction, heat convection due to tissue pores blood supply, and radiation between surface and environment [22]. Numbers of mathematical models have been constructed and applied to laser surgery, cryosurgery and cryopreservation. These models have found beneficial uses in variety of modern physiotherapy treatment, such as applying heat to the affected body part [23]. [24] measured the non-Newtonian fluid flow characteristics in micro-vessels with the effects of a magnetic field intending to obtain a high drug concentration in the target location. [25] studied numerically the impact of magnetic intensity on blood velocity at various temperatures viscosity. They found that the use of magnetic fields to control blood supply can be implemented during operations. Additionally, they considered heat transfer research in blood flow and showed that the heat transfer rate could be controlled significantly by magnetic field.

Many scientists, engineers, mathematicians, and researchers have analyzed Casson's fluid flow analysis based on different circumstances. [26] examined analytically the pulsatile blood flow via Casson fluid model in inclined artery under stenotic condition due to magnetic field. [27] investigated the blood flow problem under the effects of stenosis and particle concentration. The circulating blood is known to be Casson fluid model, and the arterial wall is considered as axisymmetrical, with an outline of the stenosis obtained by casting a slightly stenosed artery. The periodic external body acceleration effect was treated to investigate the problem of pulsatile blood flow. [28] modelled the blood as a Casson fluid to examine the blood flow in constricted narrow arteries. [29] developed a mathematical model to examine blood supply in small arteries with slight bell-shaped stenosis at low shear concentrations. Blood is viewed as a Casson fluid model. [30] considered the blood flow problem through porous arteries as Casson fluid model by utilising a fractional-order time derivative with the effects of heat transfer, thermal radiation, body acceleration and blood concentration under the effect of magnetic field.

Caputo-Fabrizio fractional derivative with a parameter memory has the advantage that the definition is not singular. Significant transforms (such as Laplace, finite Hankel, and Bessel transforms) are combined with Robotnov-Hartley functions to create a single closed-form solution for both local and non-local cases. The most crucial benefit of modelling with fractional-order derivatives is that it is non-local, which makes it different from the local model. Non-integer order derivatives, like half-order derivatives, are used to show this, with integer-order derivatives like first-order derivatives, second-order derivatives, and so on. The local model represents the system's current stage, while the non-local model describes the system's history stage. According to [32] fractional differential equations stand out from other models because of their non-local property. Other models predict a system's future stage based on its historical context and do not depend on the system's current state. According to [33] and [34], in applied mathematics, fractional calculus is a topic about derivatives or integrals of arbitrary orders (real or complex numbers). It has recently acquired prominence and appeal, and become part of well-established method of solution in science and engineering. This encompasses fluid flow issue modelling, reaction-diffusion, relaxation and dynamical processes, chemical physics, electrochemistry, electric networks, seismic wave propagation, rheology, oscillation, anomaly and turbulence, polymer and many other complex physical systems. Some works utilising fractional derivatives are conducted by [35], [36] and [37]. The effect of slip on electroosmotic flow between two plates was investigated by [35] and [37] in a second grade fluid and Oldroyd-B fluid, respectively. While, [36] examined the convective flows of a linearly viscous fluid near a plate with constantly heated and vertically located. [38] analyzed the blood flow through a stenosed permeable artery then later extended by [39] with the inclusion of hybrid nanoparticle with the effect of electroosmotic parameter. Recently, [40] and [41] studied analytically the non-Newtonian fluid flow through an elliptical duct and multi-stenosed elliptical artery, respectively. [40] concluded that the flow velocity of pseudoplastic fluid is more prominent than dilatant fluid in the vicinity of the centerline. While, [41] found that the shape of various stenosis affects the shape of contours of streamlines.

Experimental, theoretical and analytical studies of thermal radiation effects in the vascular system are scarce in the published literature. Reliable thermal radiation and Caputo-Fabrizio fractional derivative in an inclined artery have not been explored. There is an immediate need to apply with the application of fractional differential equations to the literature on thermal radiation. The goal of the current study is to extend the work of [30] by focusing on the thermal radiation effects for the Casson blood flow with the influence of magnetic particle in inclined artery. The fractional-time derivative is employed in this research to represent the Casson fluid model. The radial direction is considered in the r-axis normal outward from the center of the artery. While, the axial direction is taken into account in the z-axis along the blood flow. The body's acceleration in the z-axis, the pressure gradient, and the external magnetic force result the blood flow in the artery. The first-order derivatives for blood flows, the magnetic particle velocity, and the energy equations are converted to Caputo-Fabrizio approach in the fractional derivative models. The analytical solutions are obtained with the aid of the Laplace transformations and the finite Hankel transformation. The graphical results from the for numerical computations are obtained using Mathcad for various values of some physical parameters via Bessel functions of order zeros.

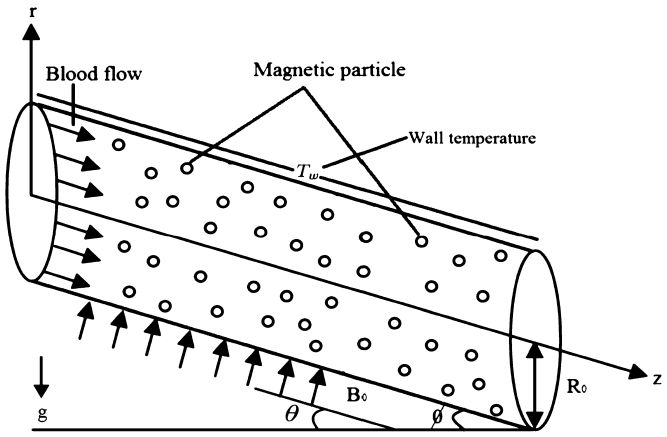

Fig. 1. Geometry configuration of an inclined artery with thermal radiation effect.

2. Formulation of the problem

In the present study, the unstable blood flow occurs in an inclined artery with a radius of R_0, where the axial direction is in the z-axis and the radial direction is in the r-axis (Fig. 1). Blood is considered to be an incompressible non-Newtonian Casson fluid. External magnetic forces, thermal radiation, and body acceleration influence the blood movement in the artery. The induced magnetic effect is believed to be negligibly weak.

The governing flow equations in cylindrical coordinate system (under the above assumptions) with the aid of the Maxwell equation, which describes the magnetic field, the Navier-Stokes' equation, which describe the motion of the blood, and the Newton's second law, which describes motion of the particle, are given as follows:

Firstly, the magnetic field in the form of Maxwell relations are [9]

$$\nabla \cdot \overrightarrow{B} = 0,\ \nabla \times \overrightarrow{E} = -\frac{\partial \overrightarrow{B}}{\partial t},\ \nabla \times \overrightarrow{B} = \mu_0 \overrightarrow{J},$$

where, the current density $\overrightarrow{J}$ is given by [31]

$$\overrightarrow{J} = \sigma\left(\overrightarrow{E} + \overrightarrow{V} \times \overrightarrow{B}\right).$$

Here, $\overrightarrow{E}$ is the electric field intensity, μ_0 is the magnetic permeability, $\overrightarrow{V}$ is the velocity vector, $\overrightarrow{B}$ is the magnetic flux intensity and σ is the electrical conductivity. The electromagnetic force $\overrightarrow{F}_{em}$ to be considered in the momentum equations is defined as [42]

$$\overrightarrow{F}_{em} = \overrightarrow{J} \times \overrightarrow{B} = -\sigma\, B_0^2\, u(r,t)\vec{k},$$

where u is the blood axial velocity, B_0 is the magnetic field strength with an inclination θ, and $\vec{k}$ is the corresponding unit vector.

The associated body acceleration is given by [44]

$$F(t) = A_g \cos(\varphi + \omega_g t),$$

where A_g is the amplitude generated by the body acceleration, φ is the phase angle and ω_g is the frequency.

The pulsatile pressure gradient due to the heart's pumping motion is given in the form [43]

$$-\frac{\partial p}{\partial z} = A_0 + A_1 cos(\omega_p t),$$

where A_0 and A_1 are the constant amplitude of pressure gradient of heart and the amplitude of pulsatile component, respectively which gives rise to systolic and diastolic pressures and ω_p is the pulsation frequency.

Secondly, the momentum equation can be written as [9], [30], [45], [46]

$$\frac{\partial u}{\partial t} = -\frac{1}{\rho}\frac{\partial p}{\partial z} + F(t) + \nu\left[1 + \frac{1}{\beta}\right]\left(\frac{\partial^2 u}{\partial r^2} + \frac{1}{r}\frac{\partial u}{\partial r}\right) + \frac{K\,N}{\rho}(v - u) - \frac{\sigma B_0^2 \sin\theta\, u}{\rho} + \frac{g\,\beta_T\left(T - T_\infty\right)\sin\phi}{\rho}, \tag{1}$$

where $u(r,t)$ is the blood distribution, ρ is the fluid density, ν is the fluid kinematic viscosity, β is the Casson parameter associated to the viscosity of Casson fluid, $\frac{KN}{\rho}(v - u)$ is the generated force subject to the relative movement of magnetic particles and the fluid itself. In this term, N is the number of magnetic particles per unit volume and K is the Stokes constant, $v(r,t)$ is the magnetic particle velocity in z-direction, $T(r,t)$ is the temperature of blood, ϕ is the inclination angle, g is the acceleration due to gravity, and β_T is the coefficient of thermal expansion. Now, the force between the magnetic particles is proportional to the relative velocity if the relative velocity has a low Reynolds number.

Finally, the Newton's second law to describe the dynamic of magnetic particle is given by [48]

$$m\frac{\partial v}{\partial t} = K\,(u - v), \tag{2}$$

where m denotes the magnetic particle's average mass.

The thermal radiation impacts on the energy equation can now be written as [30]

$$\frac{\partial T}{\partial r} = \frac{k}{\rho c_p}\left[\frac{\partial^2 T}{\partial r^2} + \frac{1}{r}\frac{\partial T}{\partial r}\right] - \frac{1}{\rho c_p}\frac{\partial q}{\partial r} + \frac{Q_m + \theta_m}{\rho c_p}, \tag{3}$$

where k is the thermal conductivity, c_p is the specific heat, Q_m is the metabolic heat source and θ_m is the heat absorption. In the current study, the non-Newtonian Casson blood is assumed as an optically thin fluid with low relative density and heat absorption coefficient $\alpha_1 \ll 1$. Thus, the heat flux can be formulated as [30]

$$-\frac{\partial q_r}{\partial r} = 4\alpha_1^2\left(T - T_\infty\right),$$

where $\alpha_1^2 = \int_0^\infty \eta\chi\frac{\partial \beta}{\partial T}$, where η, χ and β are the radiation absorption coefficient, the frequency and the Planck's constant.

The initial and boundary conditions are as follows,

$$\begin{aligned} &u(r,0) = \ v(r,0) = 0,\ T(r,0) = 0, \quad \text{at } t = 0, \quad r \in [0, R_0],\\ &u(R_0,t) = \ v(R_0,t) = 0,\ T(R_0,t) = T_w, \quad t > 0. \end{aligned} \tag{4}$$

Introducing the non-dimensional parameters

$$\begin{aligned} &r^* = \frac{r}{R_0}, t = \frac{u_0\, t}{R_0}, u^* = \frac{u}{u_0}, v^* = \frac{v}{u_0}, p^* = \frac{p}{\rho u_0^2}, z^* = \frac{z}{R_0}, A_g^* = \frac{R_0\, A_g}{u_0^2},\\ &T^* = \frac{T - T_w}{T_w - T_\infty}, Q_m^* = \frac{R_0\, Q_m}{u_0\, \rho c_p\,(T_w - T_\infty)}, \theta_m^* = \frac{R_0\, \theta_m}{u_0\, \rho c_p\,(T_w - T_\infty)}, \end{aligned} \tag{5}$$

where R_0 is the radius of artery and considered constant, u_0 is the average velocity of blood, and T_w is the wall temperature.

By using the above non-dimensional variables, the governing equations (1)-(3) (after dropped the *) becomes

$$\frac{\partial u}{\partial t} = A_0 + A_1\cos(\omega_p t) + A_g\cos(\omega_g t + \varphi) + \frac{1}{Re}\left[1 + \frac{1}{\beta}\right]\left[\frac{\partial^2 u}{\partial r^2} + \frac{1}{r}\frac{\partial u}{\partial r}\right] - Ha^2\, u + R(v - u) + Gr\, T\,\sin\phi, \tag{6}$$

$$G\,\frac{\partial v}{\partial t} = u - v, \tag{7}$$

$$Pe\frac{\partial T}{\partial t} = \left(\frac{\partial^2 T}{\partial r^2} + \frac{1}{r}\frac{\partial T}{\partial r}\right) + R_p\, T + Pe\left(Q_m + \theta_m\right), \tag{8}$$

where the Prandtl number $Pr = \frac{\mu\, c_p}{k}$, Reynolds number $Re = \frac{R_0\, u_0}{\nu}$, particle concentration parameter, $R = \frac{R_0\, K\, N}{u_0\, \rho}$ Hartmann number $Ha^2 = \frac{\sigma\, B_0^2\,\sin\theta\, R_0}{\rho u_0}$, Grashof number $Gr = \frac{g\,\beta_T\,(T_w - T_\infty)R_0}{u_0^2}$, Peclet number $Pe = Re\cdot Pr$ and the radiation parameter $R_p = \frac{4\,\alpha_1^2\, R_0^2}{k}$.

Substituting equation (5) into equation (4) results the non-dimensional boundary conditions as follows

$$\begin{aligned} &u(r,0) = \ v(r,0) = 0, \quad T(r,0) = 0, \quad r \in [0,1],\\ &u(1,t) = \ v(1,t) = 0, \quad T(1,t) = 0, \quad t > 0. \end{aligned}$$

The ordinary time derivative to Caputo-Fabrizio fractional derivative from the equations (6)-(8) are as follows,

$$\begin{aligned} &D_t^\alpha\, u = A_0 + A_1\cos(\omega_p t) + A_g\cos(\omega_g t + \varphi) + \left[1 + \frac{1}{\beta}\right]\frac{1}{Re}\left[\frac{\partial^2 u}{\partial r^2} + \frac{1}{r}\frac{\partial u}{\partial r}\right] - Ha^2\, u + R(v - u) + Gr\, T\,\sin\phi,\\ &G\, D_t^\alpha\, v = u - v,\\ &Pe\, D_t^\alpha T = \left(\frac{\partial^2 T}{\partial r^2} + \frac{1}{r}\frac{\partial T}{\partial r}\right) + R_p\, T + Pe\left(Q_m + \theta_m\right), \end{aligned}$$

where the Caputo-Fabrizio fractional time derivative [8] is given by

$$D_t^\alpha\, f(r,t) = \frac{1}{(1-\alpha)}\int_0^\tau exp\left(\frac{-\alpha(\tau - t)}{1 - \alpha}\right) f'(\tau)dt, \tag{9}$$

where α is the fractional order parameter, $(0 < \alpha < 1)$. It is known that fractional-order model is a generalisation of the integer-order model. The irregular dynamics of flow behaviour in the diffusion phenomenon have a better physical explanation due to the fractional-order model analysis. Thus, fractional model is able to provide additional information on flow phenomena that an integer-order model cannot provide. Taking the Laplace transform equation (9) results

$$L\{D_t^{\alpha} f(r,t)\} = \frac{sL\{u(r,t)\} - u(r,0)}{(1-\alpha)s + \alpha}.$$

3. Solution procedure

The Laplace transformation works well when the blood flow model uses the temporal variable t. Based on Laplace transformation on the governing equations together with the initial conditions, the following equation can be formulated as

$$\frac{s\,u(r,s)}{s+(1-s)\alpha} = A_0 + A_1\cos(\omega_p t) + A_g\cos(\omega_g t+\varphi) + \frac{1}{Re}\left[1+\frac{1}{\beta}\right]\left[\frac{\partial^2 u(r,s)}{\partial r^2} + \frac{1}{r}\frac{\partial u(r,s)}{\partial r}\right] - Ha^2\,u(r,s) + R(v(r,s) - u(r,s) + GrT(r,s)\sin\phi, \tag{10}$$

$$G\frac{s\,v(r,s)}{s+(1-s)\alpha} = u(r,s) - v(r,s), \tag{11}$$

$$\frac{s\,Pe}{s+(1-s)\alpha}T(r,s) = \left(\frac{\partial^2 T}{\partial r^2} + \frac{1}{r}\frac{\partial T}{\partial r}\right) + R_p T + Pe\left(Q_m + \theta_m\right),$$
$$u(1,s) = v(1,s) = 0,\ T(1,s) = 0. \tag{12}$$

From equation (11), results

$$v(r,s) = \frac{s+(1-s)\alpha}{(1+G)s+(1-s)\alpha}u(r,s). \tag{13}$$

Substituting $v(r,s)$ from equation (13) into equation (10) can be formulated

$$\left[\frac{s}{s+(1-s)\alpha} - R\left(\frac{s+(1-s)\alpha}{(1+G)s+(1-s)\alpha}\right) + Ha^2 + R\right]u(r,s) = \frac{A_0}{s} + \frac{A_1\,s}{s^2+\omega_p^2} + \frac{A_g\left(s\cos\varphi + \omega_g\sin\varphi\right)}{\omega_g^2+\varphi^2} + \frac{1}{Re}\left(1+\frac{1}{\beta}\right)\left(\frac{\partial^2 u}{\partial r^2} + \frac{1}{r}\frac{\partial^2 u}{\partial r}\right) + GrT(r,s)\sin\phi, \tag{14}$$

Further, applying the finite Hankel transform zeroth-order subject to boundary conditions (12) in equation (14), obtain

$$\left[\frac{s}{s+(1-s)\alpha} - R\left(\frac{s+(1-s)\alpha}{s+Gs+(1-s)\alpha}\right) + Ha^2 + R\right]u_H(r_n,s) = \left[\frac{A_0}{s} + \frac{A_1\,s}{s^2+\omega_p^2} + \frac{A_g\left(s\cos\varphi+\omega_g\sin\varphi\right)}{\omega_g^2+\varphi^2}\right]\frac{J_1(r_n)}{r_n} - \frac{1}{Re}r_n\,u_H(r_n,s) + GrT(r_n,s)\sin\phi, \tag{15}$$

$$\frac{Pe\,s}{s+\alpha(1-s)}T_H(r_n,s) = -r_n^2\,T_H(r_n,s) + R_p\,T_H(r_n,s) + \frac{Pe\left(Q_m+\theta_m\right)}{s}\frac{J_1(r_n)}{r_n}. \tag{16}$$

Here $u_H(r_n,s) = \int_0^1 r\,u(r,s)\,J_0(r_n,r)\,dr$ is the finite Hankel transform of the velocity $u(r,s) = LT[u(r,t)]$ and r_n, $n = 1,2,\ldots$ are the positive roots of the equation $J_0(x) = 0$, where J_0 represents the Bessel function of zeroth-order. By reducing the coefficient of $u_H(r_n,s)$ and $T_H(r_n,s)$ in equations (15) and (16), the following equations can be obtained

$$u_H(r_n,s) = \left[\frac{s^2x_{5n} + s\,x_{6n} + \alpha^2}{s^2x_{2n} + s\,x_{3n} + x_{4n}}\right]\left[\left(\frac{A_0}{s} + \frac{A_1\,s}{s^2+\omega_p^2} + \frac{A_g\left(s\cos\varphi+\omega_g\sin\varphi\right)}{\omega_g^2+\varphi^2}\right)\frac{J_1(r_n)}{r_n} + GrT_H(r_n,s)\sin\phi\right], \tag{17}$$

$$T_H(r_n,s) = \left[\left(\frac{Pe(Q_m-\theta_m)}{x_{12n}}\right)\left(\frac{(1-\alpha)}{s+x_{13n}} + \alpha\frac{s^{-1}}{s+x_{13n}}\right)\right]\frac{J_1(r_n)}{r_n}. \tag{18}$$

From equations (17) and (18), we get

$$u_H(r_n,s) = \left[\frac{x_{5n}}{x_{2n}} + \frac{x_{9n}}{s-x_{7n}} + \frac{x_{10n}}{s-x_{8n}}\right]\left[\left(\frac{A_0}{s} + \frac{A_1\,s}{s^2+\omega_p^2} + \frac{A_g\left(s\cos\varphi+\omega_g\sin\varphi\right)}{\omega_g^2+\varphi^2}\right) + \frac{GrPe(Q_m-\theta_m)\sin\phi}{x_{12n}}\left((1-\alpha)\frac{1}{s+x_{13n}} + \alpha\frac{s^{-1}}{s+x_{13n}}\right)\right]\frac{J_1(r_n)}{r_n}, \tag{19}$$

and rearrange equation (19) as

$$u_H(r_n,s) = \frac{J_1(r_n)}{r_n}\left[\frac{x_{5n}}{x_{2n}}\left(\frac{A_0}{s} + \frac{A_1\,s}{s^2+\omega_p^2} + \frac{A_g\left(s\cos\varphi+\omega_g\sin\varphi\right)}{\omega_g^2+\varphi^2}\right) + \frac{s^{-1}}{s-x_{7n}}A_0\,x_{9n} + \frac{s^{-1}}{s-x_{8n}}A_0\,x_{10n} + \left(\frac{1}{s-x_{7n}}\right)\left(\frac{s}{s^2+\omega_p^2}\right)A_1\,x_{9n} + \left(\frac{1}{s-x_{8n}}\right)\left(\frac{s}{s^2+\omega_p^2}\right)A_1\,x_{10n}\right.$$

$$+\left(\frac{1}{s-x_{7n}}\right)\left(\frac{s}{s^2+\omega_g^2}\right)A_g\cos\varphi\, x_{9n}-\left(\frac{1}{s-x_{7n}}\right)\left(\frac{\omega_g}{s^2+\omega_g^2}\right)A_g\sin\varphi\, x_{9n}$$
$$+\left(\frac{1}{s-x_{8n}}\right)\left(\frac{s}{s^2+\omega_g^2}\right)A_g\cos\varphi\, x_{10n}-\left(\frac{1}{s-x_{7n}}\right)\left(\frac{\omega_g}{s^2+\omega_g^2}\right)A_g\sin\varphi\, x_{10n}$$
$$+Gr\,\frac{Pe(Q_m-\theta_m)\sin\phi}{x_{12n}}\left[\frac{1}{s-x_{7n}}\frac{1}{s+x_{13n}}(1-\alpha)x_{9n}\right]+\frac{1}{s-x_{7n}}\frac{s^{-1}}{s+x_{13n}}\alpha x_{9n}$$
$$+\frac{1}{s-x_{8n}}\frac{1}{s+x_{13n}}(1-\alpha)x_{10n}+\frac{1}{s-x_{8n}}\frac{s^{-1}}{s+x_{13n}}\alpha x_{10n}\Bigg], \tag{20}$$

where

$$x_{1n}=Ha^2+R+\frac{r_n^2(1+\frac{1}{\beta})}{Re},$$
$$x_{2n}=1+G-\alpha-R-R\alpha^2+2R\alpha+x_{1n}+\alpha^2x_{1n}-2\alpha x_{1n}+Gx_{1n}-G\alpha x_{1n},$$
$$x_{3n}=\alpha+2R\alpha^2-2R\alpha-2x_{1n}\alpha^2+2\alpha x_{1n}+G\alpha,x_{1n},\quad x_{4n}=\alpha^2\,x_{1n}-R\alpha^2,$$
$$x_{5n}=1+\alpha^2-2\alpha+G-G\alpha,\qquad x_{6n}=-2\alpha^2+2\alpha+G\alpha,$$
$$x_{7n}=\frac{-x_{3n}+\sqrt{x_{3n}^2-4x_{2n}x_{4n}}}{2x_{2n}},\qquad x_{8n}=\frac{-x_{3n}-\sqrt{x_{3n}^2-4x_{2n}x_{4n}}}{2x_{2n}},$$
$$x_{9n}=\frac{x_{7n}\left(x_{6n}-\frac{x_{3n}x_{5n}}{x_{2n}}\right)+\frac{x_{4n}x_{5n}}{x_{2n}}+\alpha^2}{x_{7n}-x_8n},\qquad x_{10n}=\frac{x_{8n}\left(x_{6n}-\frac{x_{3n}x_{5n}}{x_{2n}}\right)+\frac{x_{4n}x_{5n}}{x_{2n}}+\alpha^2}{x_{8n}-x_7n},$$
$$x_{11n}=r_n^2-R_p,\quad x_{12n}=Pe+x_{11n}+\alpha\,x_{11n},\quad x_{13n}=\frac{\alpha\,x_{m11n}}{x_{12n}}.$$

Inverse Laplace transform of function $u_H(r_n,s)$ in equation (20) is formulated by applying the Hartley's and Robotnov functions

$$\mathcal{L}^{-1}\left[\frac{1}{s^w+y}\right]=F_w(-y,t)=\sum_{n=0}^{\infty}\frac{(-y)^n t^{(1+n)w-1}}{\Gamma[(1+n)w]},w>0,$$
$$\mathcal{L}^{-1}\left[\frac{s^z}{s^w+y}\right]=R_{w,z}(-y,t)=\sum_{n=0}^{\infty}\frac{(-y)^n t^{(1+n)w-1-z}}{\Gamma[(1+n)w-z]},\ Re(w-z)>0.$$

By using inverse Laplace transform on equation (20), we obtain

$$u_H(r_n,t)=\frac{J_1(r_n)}{r_n}\left[y_{1n}t+y_{2n}t+y_{3n}t+y_{4n}t+y_{5n}t+y_{6n}t\right], \tag{21}$$

where

$$y_{1n}t=\frac{x_{5n}}{x_{2n}}\left(A_0\,\delta(t)+A_1\cos\omega_p t+A_g\cos\varphi\cos\omega_g t-A_g\sin\varphi\sin\omega_g t\right),$$
$$y_{2n}t=\frac{A_0x_{9n}}{x_{7n}}\left(e^{x_{7n}t}-1\right)+\frac{A_0x_{10n}}{x_{8n}}\left(e^{x_{8n}t}-1\right),$$
$$y_{3n}t=A_1\,x_{9n}\,e^{x_{7n}t}*\cos\omega_p t+A_1\,x_{10n}\,e^{x_{8n}t}*\cos\omega_p t,$$
$$y_{4n}t=A_g\cos\varphi\,x_{9n}e^{x_{7n}t}*\cos\omega_g t-A_g\sin\varphi\,x_{10n}e^{x_{8n}t}*\sin\omega_g t,$$
$$y_{5n}t=A_g\cos\varphi\,x_{10n}e^{x_{8n}t}*\cos\omega_g t-A_g\sin\varphi\,x_{10n}e^{x_{8n}t}*\sin\omega_g t,$$
$$y_{6n}t=\frac{Gr\,Pe(Q_m-\theta_m)\sin\phi}{x_{12n}}\Big[(1-\alpha)x_{9n}\,e^{x_{7n}t}*e^{-x_{13n}t}+(1-\alpha)\,x_{10n}\,e^{x_{8n}t}*e^{-x_{13n}t}$$
$$+(1-e^{-x_{13n}t})\left(\frac{\alpha\,x_{9n}\,e^{x_{7n}t}}{x_{13n}}+\frac{\alpha\,x_{10n}\,e^{x_{8n}t}}{x_{13n}}\right)\Big].$$

From equation (18), we obtain

$$T_H(r_n,t)=\frac{J_1(r_n)}{r_n}y_{7n}t, \tag{22}$$

where

$$y_{7n}=\frac{Pe\,(Q_m-\theta_m)}{x_{12n}x_{13n}}\left[x_{3n}(1-\alpha)e^{-x_{13n}t}-\alpha(e^{-x_{13n}t}-1)\right].$$

By inverting the finite Hankel transform in equations (21) and (22) we obtain

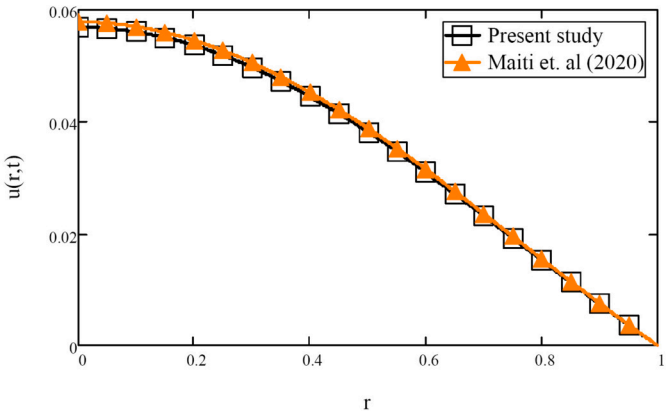

Fig. 2. Comparison of axial velocity $u(r,t)$ between Maiti et al. (2020) and present study.

$$u(r,t) = 2\sum_{n=1}^{\infty} \frac{J_0(rr_n)}{r_n J_1(r_n)} \left[y_{1n}t + y_{2n}t + y_{3n}t + y_{4n}t + y_{5n}t + y_{6n}t\right], \tag{23}$$

$$T(r,t) = 2\sum_{n=1}^{\infty} \frac{J_0(rr_n)}{r_n J_1(r_n)} y_{7n}t. \tag{24}$$

Equation (13) results the magnetic particle velocity as follows

$$\begin{aligned} v(r,s) &= \frac{s+(1-s)\alpha}{(1+G)s+(1-s)\alpha}\, u(r,s), \\ v(r,t) &= x_{14n}\left[u(r,t)\right],\ 0<\alpha<1, \end{aligned} \tag{25}$$

where

$$x_{14n} = \frac{G\,\alpha}{(1+G-\alpha^2)+\alpha}.$$

In equation (21), $f * g$ is the convolution product of f and g, and is given as

$$(f*g)(t) = \int_0^t f(\tau)\, g(t-\tau)\, d\tau.$$

4. Results and discussions

This analysis investigated the consequences of unstable Casson blood flow through an inclined artery with magnetic particles and thermal radiation. Using numerical simulations and solutions, the data related to the fractional-order parameter, x, and the other flow parameters on fluid velocity, temperature profiles, and magnetic particle distributions are presented (23), (24) and (25) with the aid of Mathcad software. The implications of fractional parameters for blood flow, magnetic particle velocity and temperature distribution have been graphically demonstrated. The effects on velocity and temperature profiles of numerous non-dimensional parameters are observed, including fractional parameters α, time t, Reynolds number Re, Hartmann number Ha, Casson fluid parameter β, radiation parameter Ra and metabolic heat supply Q_m.

For numerical computation, the values of the following parameters are fixed $A_0 = 0.05$, $A_1 = 0.05$, $G = 1$, $B_0 = 0.005$, $R = 0.5$, $Re = 10$, $\omega = \frac{\pi}{4}$, $\phi = \frac{\pi}{4}$, $t = 0.3$, $Ha = 2$, $\beta = 0.8$, $Pe = 1.5$ and $Q_m = 0.1$ as studied by [30][47]. All velocity and temperature profiles have been plotted for various fractional parameters and r values. It is obvious that the fractional parameter is important for regulating body temperature and blood pressure. The range of values of the fractional parameters is set as $\alpha \in [0,1]$. In current study, the behaviour of Casson fluids with magnetic particles that flow through an inclined artery with thermal radiation effect is considered. The current results have been compared with the results of [30] for both velocity and temperature profile having same fluid properties and thermal radiation effects as shown in Figs. 2 and 3. For the purpose of comparison, $A_0 = 0.05$, $A_1 = 0.05$, $G = 1$, $B_0 = 0.005$, $R = 0.5$, $Re = 10$, $\omega = \frac{\pi}{4}$, $\phi = \frac{\pi}{4}$, $t = 0.3$, $Ha = 2$, $\beta = 0.8$, $Pe = 1.5$ and $Q_m = 0.1$ so that both problems are in the identical configurations.

Fig. 4 shows the velocity profile of blood flow for different fractional parameter values, α. It shows that velocity increases as parameter α increased. It is notable that the fractional parameter, α, would completely affect the velocity profiles. In this case the ordinary fluid could be obtained by setting $\alpha = 1$. Fig. 5 indicates the difference in blood flow with Reynolds number. The figure shows that the velocity of blood flow steadily increases as the Reynolds number increases and becomes more flattened for the ordinary fluid. The Reynolds number shows increased blood velocity, which indicates that the strength of inertial forces within the fluid due to the apparent number of viscous forces that have been removed and resisted the flow at a limited number of Reynolds.

Fig. 6 displays the variation of Hartmann number Ha, over the blood particle motion. It can be seen from the figure that by increasing the strength of the applied magnetic field, the velocity of the magnetic particle diminished. It is clear that when the

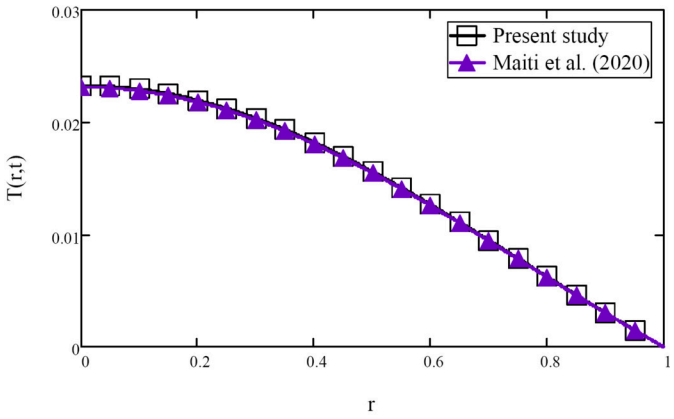

Fig. 3. Comparison of temperature profile $T(r,t)$ between Maiti et al. (2020) and present study.

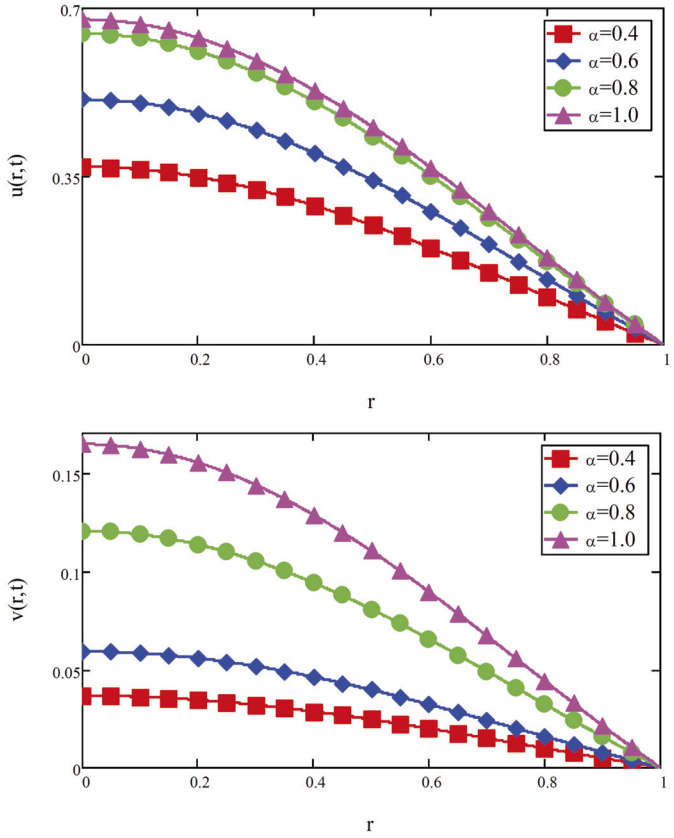

Fig. 4. Variation of axial velocities $u(r,t)$ and $v(r,t)$ for different values of fractional parameter, α.

variation of Hartman number devoted to the flow field leads to divergence of Lorentz force. It tends to produce more resistance to transport phenomena resulting in reduce axial velocity values. Casson effect is more relevant for narrow arteries where red blood cells could accumulate near the artery's axis due to rotation, forming a cell-depicted area. Fig. 7 has been plotted to clarify the effects of the Casson fluid parameter of the magnetic particle velocity. From this figure, it is evident that with an increase in the Casson parameter β, the fluid's speed increased. An increase in the Casson fluid parameter reduces the yield's tension and thus decreases the thickness of the boundary layer. Fig. 8 shows the influence of different inclination angle on velocities. Both velocities are increases with the increase of ϕ. Due to the resistive force, it is important to note that magnetic particles speed is slower than blood velocity.

Figs. 9-11 display the impact of temperature profiles for various values of the fractional parameter, radiation parameter, and metabolic heat source. The temperature distribution is significantly affected by the multiple values of the fractional parameter α, as shown in Fig. 9. It shows that the temperature decreases with an increase in the fractional parameter. This indicates that the fractional-order fluid model's temperature distribution would be much higher than the ordinary one. In Fig. 10, the temperature

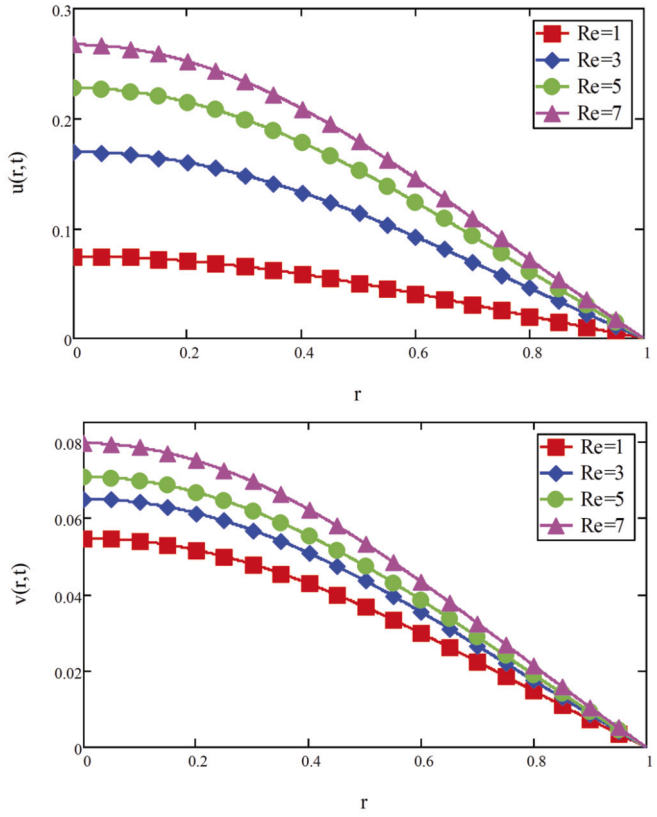

Fig. 5. Variation of axial velocities $u(r,t)$ and $v(r,t)$ for different values of Reynolds number, Re.

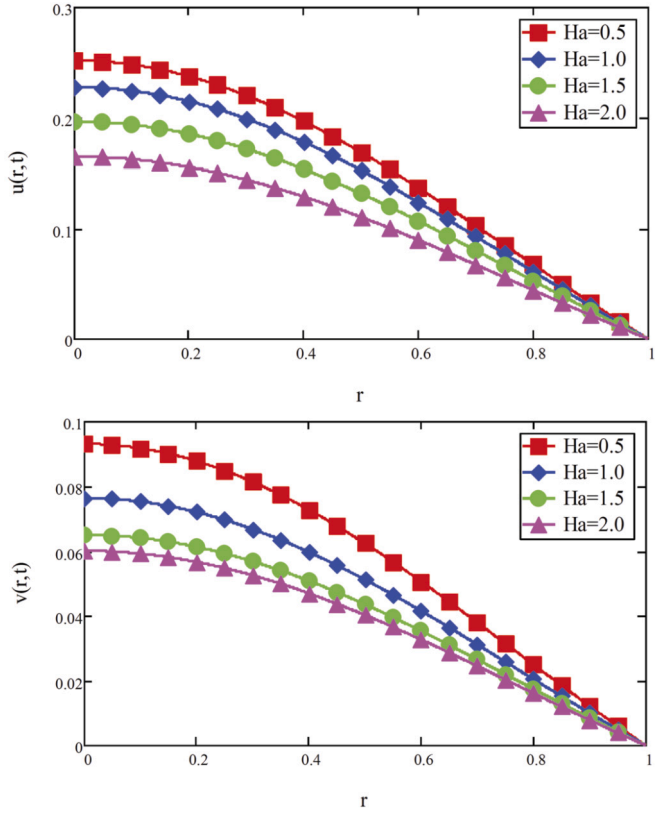

Fig. 6. Variation of axial velocities $u(r,t)$ and $v(r,t)$ for different values of Hartmann number, Ha.

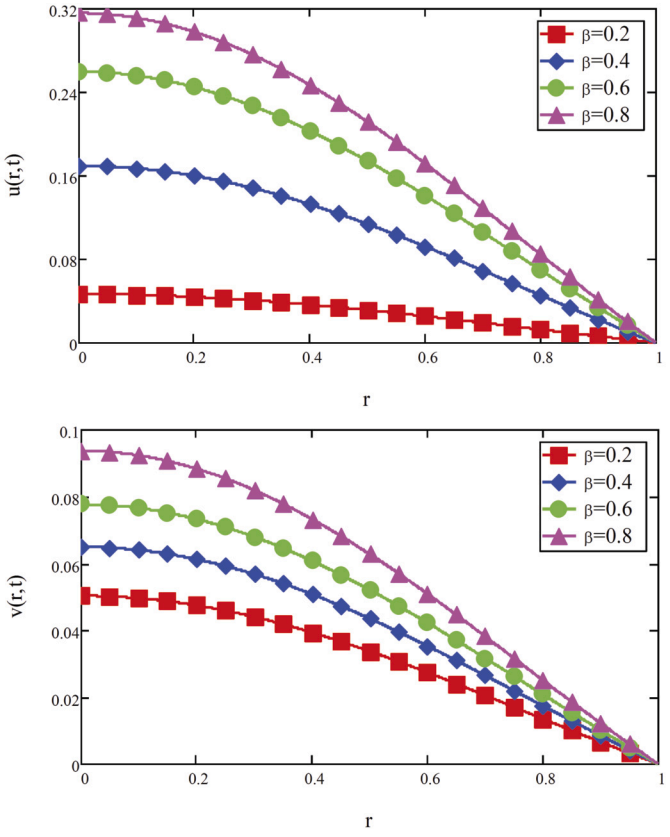

Fig. 7. Variation of axial velocities $u(r,t)$ and $v(r,t)$ for different values of Casson parameter β.

profiles for various radiation parameters are presented. Temperature amplitude changes as the thermal radiation increases. The central line has enhanced temperature. During hyperthermia, this temperature spread is particularly essential; the inner blood temperature rises without impacting the underlying blood vessel tissue. Fig. 11 shows the results for small variation values of metabolic heat sources Q_m to the temperature profile. With the help of metabolic heat parameters within the bloodstream, additional heat is produced to regulate internal body temperature. When the metabolic heat sources increases, the temperature in the blood vessel increases as well. This finding confirms the results obtained in [30].

5. Conclusions

A mathematical model has been developed to analyse the fractional-order blood flow model on the non-Newtonian Casson fluid flow through an inclined artery under the influence of an external magnetic field and thermal radiation. Using the Laplace and finite Hankel transform of order zero, the mathematical model's solution is obtained. Usually, the extraction of the ordinary model involves an additional mathematical solution; however, the ordinary model for the velocity equation can be obtained directly using the present technique, since the equation is fully compatible. The fractional parameter order significantly impacts the distributions of velocity, magnetic particles, and temperature. Blood flow motion increases as the fractional parameter, time, Reynolds number and the parameter of Casson fluid increases, and decreases as the Hartmann value increases. Additionally, fractional parameters, radiation, and metabolic heat source all play an essential role in regulating blood temperature. The findings obtained in this analysis are technically important and thus interesting to understand the drug particle concentration phenomenon for drug distribution applications.

CRediT authorship contribution statement

Dzuliana Fatin Jamil: Writing – original draft, Data curation, Conceptualization. **Salah Uddin:** Writing – original draft, Visualization, Formal analysis, Data curation. **Mohsin Kazi:** Writing – review & editing, Investigation, Funding acquisition, Formal analysis. **Rozaini Roslan:** Writing – review & editing, Writing – original draft, Supervision, Investigation, Formal analysis, Conceptualization. **M.R. Gorji:** Writing – review & editing, Writing – original draft, Methodology, Investigation, Formal analysis. **Mohd Kamalrulzaman Md Akhir:** Writing – original draft, Software, Methodology, Investigation, Conceptualization.

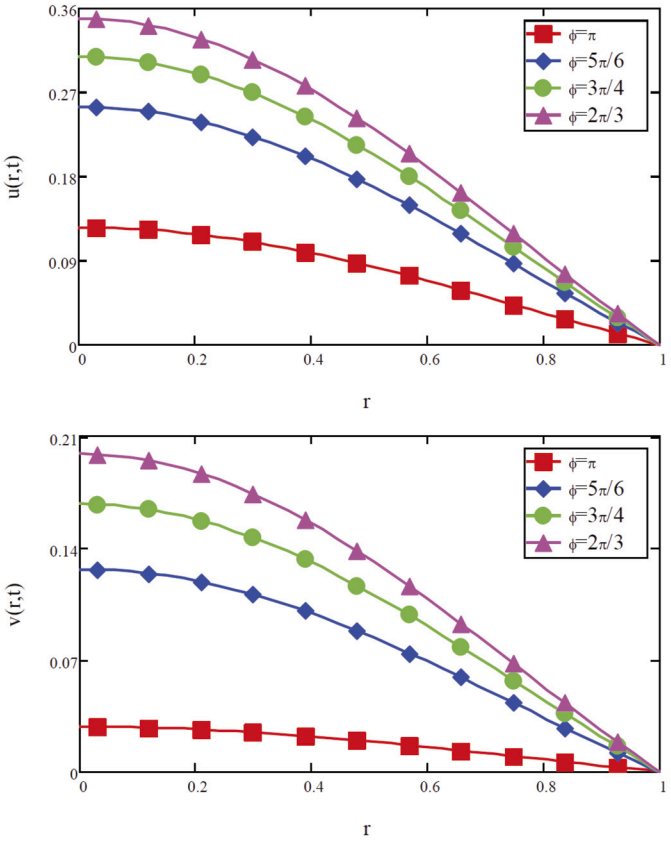

Fig. 8. Variation of axial velocities $u(r,t)$ and $v(r,t)$ for different values of inclination angle, ϕ.

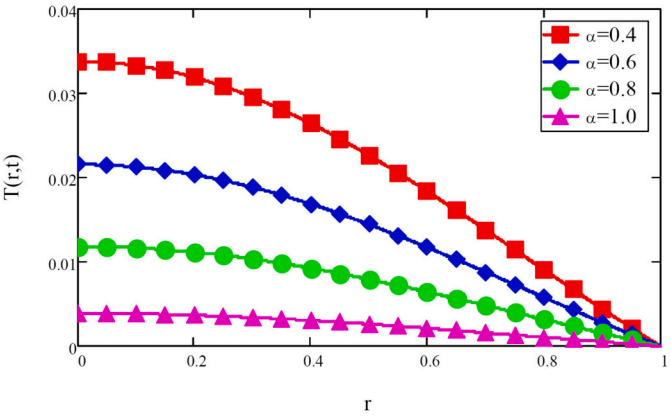

Fig. 9. Variation of temperature profile $T(r,t)$ for different values of fractional parameter, α.

Declaration of competing interest

The authors declare that they have no known competing financial interests or personal relationships that could have appeared to influence the work reported in this paper.

Data availability

No data was used for the research described in the article.

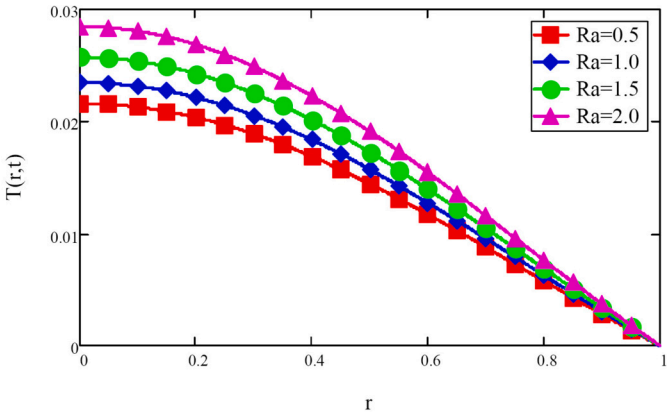

Fig. 10. Variation of temperature profile $T(r,t)$ for different values of radiation parameter, Ra.

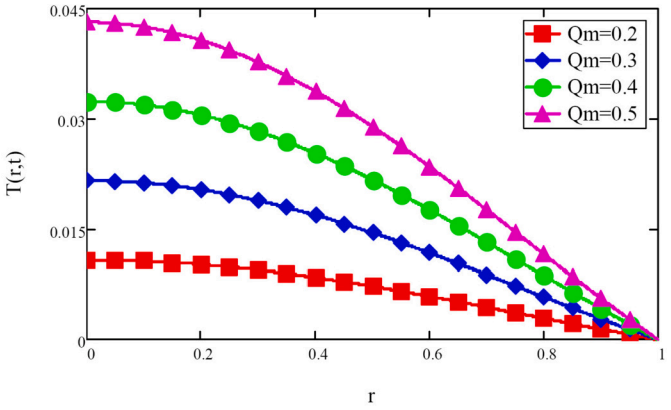

Fig. 11. Variation of temperature profile $T(r,t)$ for different values of metabolic heat source, Q_m.

Acknowledgement

The authors would like to extend their sincere appreciation to the Researchers Supporting Project Number (RSP2023R301), King Saud University, Riyadh, Saudi Arabia. Also, this research was supported by Ministry of Higher Education (MOHE) Malaysia through Fundamental Research Grant Scheme (FRGS/1/2019/STG06/UTHM/01/1) Vot No. K172.

References

[1] E.E. Tzirtzilakis, Biomagnetic fluid flow in a channel with stenosis, Phys. D: Nonlinear Phenom. 237 (1) (2008) 66–81, https://doi.org/10.1016/j.physd.2007.08.006.
[2] Ö. Türk, M. Tezer-Sezgin, C. Bozkaya, Finite element study of biomagnetic fluid flow in a symmetrically stenosed channel, J. Comput. Appl. Math. 259 (Part B) (2014) 760–770, https://doi.org/10.1016/j.cam.2013.06.037.
[3] S. Bose, M. Banerjee, Magnetic particle capture for biomagnetic fluid flow in stenosed aortic bifurcation considering particle-fluid coupling, J. Magn. Magn. Mater. 385 (2015) 32–46, https://doi.org/10.1016/j.jmmm.2015.02.060.
[4] K. Tzirakis, L. Botti, V. Vavourakis, Y. Papaharilaou, Numerical modeling of non-Newtonian biomagnetic fluid flow, Comput. Fluids 126 (2016) 170–180, https://doi.org/10.1016/j.jmmm.2015.02.060.
[5] E.E. Tzirtzilakis, A mathematical model for blood flow in magnetic field, Phys. Fluids 17 (7) (2005) 1–15, https://doi.org/10.1063/1.1978807.
[6] D. Tripathi, A mathematical model for blood flow through inclined arteries under the influence of inclined magnetic field, J. Mech. Med. Biol. 12 (3) (2012) 1–18, https://doi.org/10.1142/S0219519411004812.
[7] S.U. Siddiqui, C. Awasthi, Mathematical analysis on pulsatile flow through a catheterized stenosed artery, J. Appl. Math. Phys. 5 (9) (2017) 1874–1886, https://doi.org/10.4236/jamp.2017.59157.
[8] M. Caputo, M. Fabrizio, A new definition of fractional derivative without singular kernel, Prog. Fract. Differ. Appl. 1 (2) (2015) 73–85, https://doi.org/10.12785/pfda/010201.
[9] N.A. Shah, D. Vieru, C. Fetecau, Effects of the fractional order and magnetic field on the blood flow in cylindrical domains, J. Magn. Magn. Mater. 409 (2016) 10–19, https://doi.org/10.1016/j.jmmm.2016.02.013.
[10] S. Uddin, M. Mohamad, M.R. Gorji, R. Roslan, I.M. Alarifi, Fractional electro-magneto transport of blood modeled with magnetic particles in cylindrical tube without singular kernel, Microsyst. Technol. 26 (1) (2020) 405–414, https://doi.org/10.1007/s00542-019-04494-0.
[11] M.I. Asjad, N.A. Shah, M. Aleem, I. Khan, Heat transfer analysis of fractional second-grade fluid subject to Newtonian heating with Caputo and Caputo-Fabrizio fractional derivatives: a comparison, Eur. Phys. J. Plus 132 (8) (2017) 340, https://doi.org/10.1140/epjp/i2017-11606-6.
[12] M. Abdulhameed, D. Vieru, R. Roslan, Magnetohydrodynamic electroosmotic flow of Maxwell fluids with Caputo-Fabrizio derivatives through circular tubes, Comput. Math. Appl. 74 (10) (2017) 2503–2519, https://doi.org/10.1016/j.camwa.2017.07.040.

[13] H. Bakhti, L. Azrar, D. Baleanu, Pulsatile blood flow in constricted tapered artery using a variable-order fractional Oldroyd-B model, Therm. Sci. 21 (1) (2017) 29–40, https://doi.org/10.2298/TSCI160421237B.
[14] N.A. Shah, Y. Mahsud, A.A. Zafar, Unsteady free convection flow of viscous fluids with analytical results by employing time-fractional Caputo-Fabrizio derivative (without singular kernel), Eur. Phys. J. Plus 132 (10) (2017) 411, https://doi.org/10.1140/epjp/i2017-11711-6.
[15] M. Saqib, F. Ali, I. Khan, N.A. Sheikh, S.A.A. Jan, Samiulhaq, exact solutions for free convection flow of generalized Jeffrey fluid: a Caputo-Fabrizio fractional model, Alex. Eng. J. 57 (3) (2018) 1849–1858, https://doi.org/10.1016/j.aej.2017.03.017.
[16] F. Ali, M. Iftikhar, I. Khan, N.A. Sheikh, Aamina, K.S. Nisar, Time fractional analysis of electro-osmotic flow of Walters-B fluid with time-dependent temperature and concentration, Alex. Eng. J. 59 (1) (2020) 25–38, https://doi.org/10.1016/j.aej.2019.11.020.
[17] B. Tashtoush, A. Magableh, Magnetic field effect on heat transfer and fluid flow characteristics of blood flow in multi-stenosis arteries, Heat Mass Transf. (Waerme-und Stoffuebertragung) 44 (3) (2008) 297–304, https://doi.org/10.1007/s00231-007-0251-x.
[18] S. Chakravarty, P.K. Mandal, Effect of heat and mass transfer on non-Newtonian flow - links to atherosclerosis, Int. J. Heat Mass Transf. 52 (25–26) (2009) 5719–5730, https://doi.org/10.1016/j.ijheatmasstransfer.2009.04.040.
[19] M.Y. Malik, A. Hussain, Flow of a Jeffery-six constant fluid between coaxial cylinders with heat transfer analysis, Commun. Theor. Phys. 56 (2) (2011) 345, https://doi.org/10.1088/0253-6102/56/2/27.
[20] D.D. Ganji, A. Hamzehnezhad, A. Rahbari, M. Fakour, M.A. Vakilabadi, Heat transfer and fluid flow of blood with nanoparticles through porous vessels in a magnetic field: a quasi-one dimensional analytical approach, Math. Biosci. 283 (2017) 38–47, https://doi.org/10.1016/j.mbs.2016.11.009.
[21] K.A. Abro, M.A. Solangi, Heat transfer in magnetohydrodynamic second grade fluid with porous impacts using Caputo-Fabrizoi fractional derivatives, J. Math. 49 (2) (2017) 113–125.
[22] T. Hayat, S. Hina, A.A. Hendi, S. Asghar, Effect of wall properties on the peristaltic flow of a third grade fluid in a curved channel with heat and mass transfer, Int. J. Heat Mass Transf. 54 (23–24) (2011) 5126–5136, https://doi.org/10.1016/j.ijheatmasstransfer.2011.07.036.
[23] A. Sinha, G.C. Shit, Electromagnetohydrodynamic flow of blood and heat transfer in a capillary with thermal radiation, J. Magn. Magn. Mater. 378 (2015) 143–151, https://doi.org/10.1016/j.jmmm.2014.11.029.
[24] S. Shaw, P.V.S.N. Murthy, S.C. Pradhan, Effect of non-Newtonian characteristics of blood on magnetic targeting in the impermeable micro-vessel, J. Magn. Magn. Mater. 322 (8) (2010) 1037–1043, https://doi.org/10.1016/j.jmmm.2009.12.010.
[25] S. Majee, G.C. Shit, Numerical investigation of MHD flow of blood and heat transfer in a stenosed arterial segment, J. Magn. Magn. Mater. 424 (2017) 137–147, https://doi.org/10.1016/j.jmmm.2016.10.028.
[26] N. Srivastava, The Casson fluid model for blood flow through an inclined tapered artery of an accelerated body in the presence of magnetic field, Int. J. Biomed. Eng. Technol. 15 (3) (2014) 198–210, https://doi.org/10.1504/IJBET.2014.064646.
[27] Sarifuddin, CFD modelling of Casson fluid flow and mass transport through atherosclerotic vessels, Differ. Equ. Dyn. Syst. 30 (2) (2020) 253–269, https://doi.org/10.1007/s12591-020-00522-y.
[28] P. Nagarani, G. Sarojamma, Effect of body acceleration on pulsatile flow of Casson fluid through a mild stenosed artery, Korea Aust. Rheol. J. 20 (4) (2008) 189–196.
[29] J. Venkatesan, D.S. Sankar, K. Hemalatha, Y. Yatim, Mathematical analysis of Casson fluid model for blood rheology in stenosed narrow arteries, J. Appl. Math. 2013 (2013) 583809, https://doi.org/10.1155/2013/583809.
[30] S. Maiti, S. Shaw, G.C. Shit, Caputo-Fabrizio fractional order model on MHD blood flow with heat and mass transfer through a porous vessel in the presence of thermal radiation, Phys. A, Stat. Mech. Appl. 540 (2020) 123149, https://doi.org/10.1016/j.physa.2019.123149.
[31] M. Hatami, J. Hatami, D.D. Ganji, Computer simulation of MHD blood conveying gold nanoparticles as a third grade non-Newtonian nanofluid in a hollow porous vessel, Comput. Methods Programs Biomed. 113 (2014) 632–641, https://doi.org/10.1016/j.cmpb.2013.11.001.
[32] M. Hatami, J. Hatami, D.D. Ganji, A fractional model of Navier-Stokes equation arising in unsteady flow of a viscous fluid, J. Assoc. Arab Univ. Basic Appl. Sci. 17 (2014) 14–19, https://doi.org/10.1016/j.jaubas.2014.01.001.
[33] M. Caputo, Fractional calculas and applied analysis, Int. J. Theory Appl. 11 (1) (2008) 73–85.
[34] M. Riesz, L'integral de Riemann-Liouville et le probleme de cauchy pour l'equation des ondes, Bull. Soc. Math. Fr. 67 (1939) 153–170, https://doi.org/10.24033/bsmf.1309.
[35] A.U. Awan, M.D. Hisham, N. Raza, The effect of slip on electro-osmotic flow of a second-grade fluid between two plates with Caputo-Fabrizio time fractional derivatives, Can. J. Phys. 97 (5) (2018) 509–516, https://doi.org/10.1139/cjp-2018-0406.
[36] A.U. Awan, N.A. Shah, N. Ahmed, Q. Ali, S. Riaz, Analysis of free convection flow of viscous fluid with damped thermal and mass fluxes, Chin. J. Phys. 60 (2019) 98–106, https://doi.org/10.1016/j.cjph.2019.05.006.
[37] A.U. Awan, M. Ali, K.A. Abro, Electroosmotic slip flow of Oldroyd-B fluid between two plates with non-singular kernel, J. Comput. Appl. Math. 376 (2020) 112885, https://doi.org/10.1016/j.cam.2020.112885.
[38] M.H. Shahzad, N.A. Ahammad, S. Nadeem, S.A. Allahyani, E.M. Tag-ElDin, A.U. Awan, Sensitivity analysis for Rabinowitsch fluid flow based on permeable artery constricted with multiple stenosis of various shapes, Biomass Convers. Biorefin. (2022), https://doi.org/10.1007/s13399-022-03311-5.
[39] M.H. Shahzad, A.U. Awan, S. Akhtar, S. Nadeem, Entropy and stability analysis on blood flow with nanoparticles through a stenosed artery having permeable walls, Sci. Prog. 105 (2) (2022) 1–34, https://doi.org/10.1177/00368504221096000.
[40] M.H. Shahzad, A.U. Awan, Mechanics of heated Rabinowitsch fluid in elliptic vertical duct: peristalsis and analytical study, Int. J. Mod. Phys. B 37 (2023) 2350274, https://doi.org/10.1142/S0217979223502740.
[41] M.H. Shahzad, A.U. Awan, Non-Newtonian characteristics of blood flow in a multi-stenosed elliptical artery: a case of sensitivity analysis, Int. J. Mod. Phys. B 37 (19) (2023) 2350182, https://doi.org/10.1142/S0217979223501825.
[42] C.D. Bansi, C.B. Tabi, T.B. Motsumi, Fractional blood flow in oscillatory arteries with thermal radiation and magnetic field effects, J. Magn. Magn. Mater. 456 (2018) 38–45, https://doi.org/10.1016/j.jmmm.2018.01.079.
[43] V.K. Tanwar, N.K. Varshney, R. Agarwal, Effect of body acceleration on pulsatile blood flow through a catheterized artery, Adv. Appl. Sci. Res. 2 (2016) 155–166.
[44] G.C. Shit, M. Roy, Pulsatile flow and heat transfer of a magneto-micropolar fluid through a stenosed artery under the influence of body acceleration introduction, J. Mech. Med. Biol. 11 (3) (2011) 643–661, https://doi.org/10.1142/S0219519411003909.
[45] F. Ali, N.A. Sheikh, I. Khan, M. Saqib, Magnetic field effect on blood flow of Casson fluid in axisymmetric cylindrical tube: a fractional model, J. Magn. Magn. Mater. 423 (2017) 327–336, https://doi.org/10.1016/j.jmmm.2016.09.125.
[46] M.K. Sharma, K. Singh, S. Bansal, Pulsatile MHD flow in an inclined catheterized stenosed artery with slip on the wall, J. Biomed. Sci. Eng. 7 (4) (2014) 194–207, https://doi.org/10.4236/jbise.2014.74023.
[47] C.D.K. Bansi, C.B. Tabi, T.G. Motsumi, A. Mohamadou, Fractional blood flow in oscillatory arteries with thermal radiation and magnetic field effects, J. Magn. Magn. Mater. 456 (2018) 38–45, https://doi.org/10.1016/j.jmmm.2018.01.079.
[48] S. Sharma, U. Singh, V.K. Katiyar, Magnetic field effect on flow parameters of blood along with magnetic particles in a cylindrical tube, J. Magn. Magn. Mater. 377 (2015) 395–401, https://doi.org/10.1016/j.jmmm.2014.10.136.